STUDIES ON CELLULOSE NANOCRYSTALS EXTRACTED FROM *MUSA SAPIENTUM*: STRUCTURAL AND BONDING ASPECTS

DEBABRATA DAS,[*] SHAMIMA HUSSAIN,[**] ANUP KUMAR GHOSH[*] and ARUN KUMAR PAL[*]

[*]*Department of Instrumentation Science, Jadavpur University, Kolkata-700 032, India*
[**]*UGC-DAE CSR, Kalpakkam Node, Kokilamedu-603104, India*
✉ *Corresponding author: Arun Kumar Pal, msakp2002@yahoo.co.in*

Received May 12, 2017

Cellulose fibers were obtained from banana pseudo-stems and subjected to different treatments to achieve nanocrystals. The cellulose materials obtained after different stages of extraction were studied using X-ray diffraction (XRD), X-ray photoelectron spectroscopy (XPS), Raman spectroscopy and Fourier transform infrared spectroscopy (FTIR). XRD measurements revealed higher crystalline cellulose content in the acid hydrolyzed sample than in the raw fiber, with crystallite sizes of ~3.5 nm. XPS results indicated a significant intensity decrease of the peak located at ~285 eV, corresponding to the non-cellulosic component, in the spectrum of the raw fiber, as compared to that of the acid hydrolyzed sample. Raman studies indicated higher content of sp^2 hybridized carbon in the raw fiber, due to its high amorphous carbon content, while acid treated crystalline samples showed significantly higher sp^3 hybridized carbon content, indicating higher crystallinity. FTIR studies indicated that the raw material contained the highest amount of sp^2 bonded carbon and the acid treated crystalline samples contained the most sp^3 bonded carbon.

Keywords: cellulose nanocrystals, XRD, FTIR, XPS, Raman

INTRODUCTION

Cellulose nanocrystals (CNCs) have attracted increasing research interest due to their unique characteristics, such as large surface to volume ratio, high surface area, high Young's modulus, high tensile strength, low coefficient of thermal expansion and formation of highly porous mesh, as compared to other commercial fibers.[1] Being a fibrous polymer, cellulose is composed of large molecules in the form of long chains in the crystalline form. These chains grow side by side in regular form and intervals. The cellulose fibers consist of two regions: amorphous and crystalline regions.

Most of the studies reported so far have tackled the feasibility of extracting cellulose from different natural sources. Some of the current reports worth mentioning are described below. Chirayil *et al.*[2] carried out an extensive review of the techniques for isolating cellulose nanofibrils (CNFs). Abdullah *et al.*[3] characterized banana pseudo-stem and banana fruit-bunch-stem to obtain value-added products from them. A study on the thermal stability of crystalline cellulose was reported by Kim *et al.*[4] Rosa *et al.*[5] isolated cellulose whiskers from rice husk. They used an environmentally friendly chlorine-free process for extraction. The effects of spray-drying or freeze-drying on the chemical signatures, thermal and morphological features of CNCs have been investigated by George *et al.*[6] Hong *et al.*[7] obtained two types of CNCs from bamboo pulp by sulfuric acid hydrolysis: rods and porous networks. CNCs were directly extracted by Corradini *et al.*[8] from curaua fibers by acid hydrolysis using H_2SO_4, HCl and a mixture of the two. The effect of the acids on the thermal stability of the CNCs was evaluated by thermogravimetric studies. Feng *et al.*[9] reported an environment-friendly process to prepare CNFs from sugarcane bagasse by combining ultrasonication with various mechanochemical pretreatments. They observed that individual CNFs had diameters of ~20-40 nm with high aspect ratios, a fine web-like structure and good

thermal stability. Despite the efforts made during the last decade or so for characterizing celluloses obtained from different resources, a comprehensive report on structural and bonding aspects of cellulose obtained during different extraction stages seems to be relevant even today.

In this report, the structure and the bonding environment in cellulose fibrils during different stages of extraction have been studied critically using conventional physical and chemical methods. Fibrils were characterized by evaluating their microstructural properties using field emission scanning electron microscopy (FESEM) and X-ray diffraction (XRD). X-ray photoelectron spectroscopy (XPS), Fourier transform infrared spectroscopy (FTIR) and Raman studies were also carried out to obtain information on the modulation of the bonding environment in the raw material, as it undergoes modifications after each successive chemical treatment to reach the final crystalline stage. Such a systematic study would provide a clearer insight into the modifications of the bonding environment in these fibers during successive extraction stages.

EXPERIMENTAL

Banana pseudo-stems (*Musa sapientum* L.) were collected from local cultivators. Pseudo-stem fibers were isolated from the outer layers manually in the laboratory and washed immediately in distilled water to remove dirt and residues. The fibers were dried at room temperature and stored for further experimentation. The thus obtained raw materials are henceforth referred to as BFR in this article. This BFR was subjected to various treatments, such as alkali treatment, bleaching and acid hydrolysis, to obtain cellulose materials designated as BFS, BFB and BFA, respectively. The raw banana fibers were cut into small pieces of approximately 3-5 cm. Alkali treatment was carried out using the steam explosion method. In this method, 2% NaOH was added to the fibers placed in an autoclave operated at a pressure of ~20 lb and temperature of ~110-120 °C for a period of 1 h. The fibers were then thoroughly washed several times with distilled water until pH neutrality was reached. This process was repeated three times. Then, an air oven operated at ~105 °C was used to dry the fibers for a total time of ~4 h. The alkali treated fiber samples obtained as described above were then subjected to bleaching to remove the remaining lignin. The bleaching process was carried out with a 1.7 wt% sodium hypochlorite solution at 60-70 °C for 4 hours with constant stirring. Glacial acetic acid was used as buffer to maintain the pH of the solution at ~4.5-6.5. The mixture was allowed to cool and then was filtered. The residue was then washed with distilled water. The bleached sample obtained as mentioned above was then acid hydrolyzed with a 10(M) H_2SO_4 solution at the temperature of ~50 °C for 40 minutes under constant stirring. Excess water was added to terminate the reaction. The residue was then washed by repeated centrifugation. Finally, the sample was dried in the oven at ~105 °C to obtain CNCs. All the chemicals used here were purchased form Merck India Ltd.

The CNCs obtained as described above were characterized by XRD, using a Rigaku MiniFlex XRD system (CuKα line, 0.154 nm, 30 kV and 20 mA), in the 2θ range between 10° and 40°. All the samples were ground to powder. Pellets made from the above-mentioned powders were used for XPS and Raman measurement. Al Kα at 1486.74 eV was used as X-ray source to record the XPS spectra by an M/S SPECS spectrophotometer (Germany), with a PHOIBOS HSA3500 analyzer and a DLSEGD 150 R7 detector. A Renishaw inVia micro-Raman spectrometer (785 nm Diode laser) was used for Raman studies. FTIR spectroscopy was performed with a Shimadzu FTIR-8400S Spectrophotometer over the range of 400-4000 cm^{-1}. Surface morphology was studied by a field emission scanning electron microscope (Inspect S50, FEI) at an operating voltage of 3 kV in secondary emission mode.

RESULTS AND DISCUSSION

Microstructural studies

Cellulosic materials obtained after different stages of extraction contain different amounts of amorphous and crystalline portions. XRD measurements would provide a preview of the relative ratio of the amorphous to the crystalline regions of the cellulose material present in the above extracts.

Numerous techniques have been adopted for determining crystallinity.[10-13] However, X-ray diffraction techniques are the most widely used ones. The term crystallinity index (CI) was introduced by Segal *et al*. and was used for rapid determination of the relative crystallinity of cellulose by the peak height method.[14] However, recently, Driemeier and Calligaris[15] indicated that associating peak height with the degree of crystallinity, as proposed in Segal's method, may not be appropriate to represent the experimental data faithfully, whereas, the peak areas under the above peaks would be more a realistic representation of CI. Both methods have their own merits and demerits. We would like to emphasize here that the area covered under the peaks of the crystalline and amorphous phases may not be the best parameter to use since it is essentially equivalent to the product of the intensity ratio (I_{cr}/I_{am}) and FWHM. Thus, it will

be interesting to study the dependence of the crystalline index factor on I_{cr}/I_{am} and the area covered under the peaks separately, since they may contain different information. We have compared the crystallinity index calculated using both methods. Recently, a comprehensive analysis of the methods for representing CI from XRD data has been reported by French[16] and French *et al.*[17] It has been inferred that reliable determinations of the crystal structure coordinates of the various polymorphs are still highly necessary for better understanding the structural aspects of cellulose. There is a real need for a more faithful report on the structural analysis of cellulose.

The XRD traces of all the materials obtained during different stages of extraction are shown in Figure 1 (a-d), while the corresponding insets show the FESEM pictures of the same material. It may be observed that all the spectra contained peaks located at 2θ~14.9°, 2θ~16.7°, 2θ~22.6° and 2θ~34.9° corresponding to peaks arising due to reflections from (1$\bar{1}$0), (110), (200) and (004) planes of cellulose I, respectively.[18-21] The variation of peak intensity and of the area under the peaks is associated with distinct structural changes in the materials after different extraction stages. BFR exhibited the lowest intensity (Fig. 1 (a)) for all the peaks. The intensity of the peaks increased (Fig. 1 (b)) for BFS. The inset of Figure 1 (b) shows the FESEM picture of the BFS sample. The SEM images also reveal that the skeleton consists mainly of cellulose. Mostly, ribbon-like filaments can be observed in the BFS samples (Fig. 1 (b)). An improvement in the bonding inside the structure due to external fibrillation could be expected due to the above ribbon-like filaments. One may observe that the intensity of the XRD peaks increased after the bleaching treatment of the samples (BFB) (Fig. 1 (c)). The intensities of the peaks are higher than those for the alkali treated samples (BFS). The acid treated samples (BFA) had the highest intensities for all the peaks (Fig. 1 (d)). The peaks showed a slight shift in position towards lower values of 2θ, as evident from Figure 1 (a-d), representing the characteristic peaks for the crystal form of the cellulose I polymorph (Table 1). A similar behavior has been reported in other studies.[19,22] Changes in the morphology caused by the effects of various treatments on the raw fiber, at different stages of extraction, are apparent from the SEM images of banana fibers (insets of Fig. 1 (a-d)). These micrographs indicate that, after the acid treatment, the skeleton of the fiber and its surrounding layer are partly destroyed (inset of

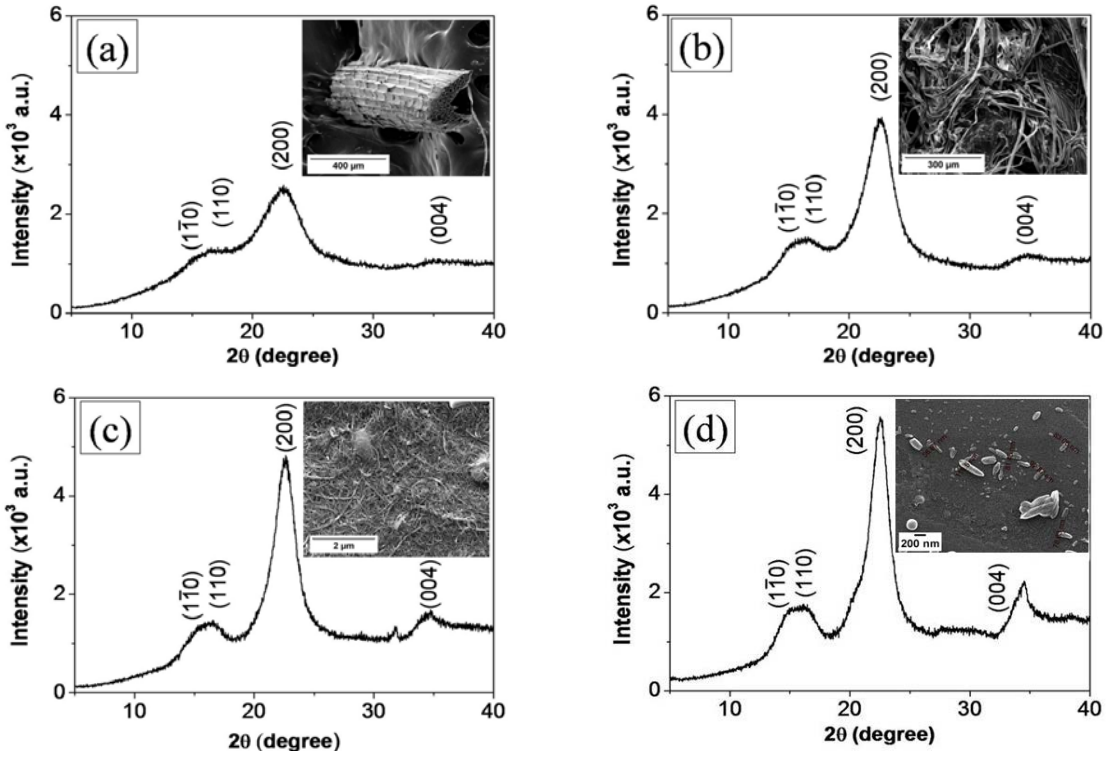

Figure 1: XRD patterns of banana fibers: (a) BFR, (b) BFS, (c) BFB and (d) BFA
(insets show the corresponding FESEM pictures)

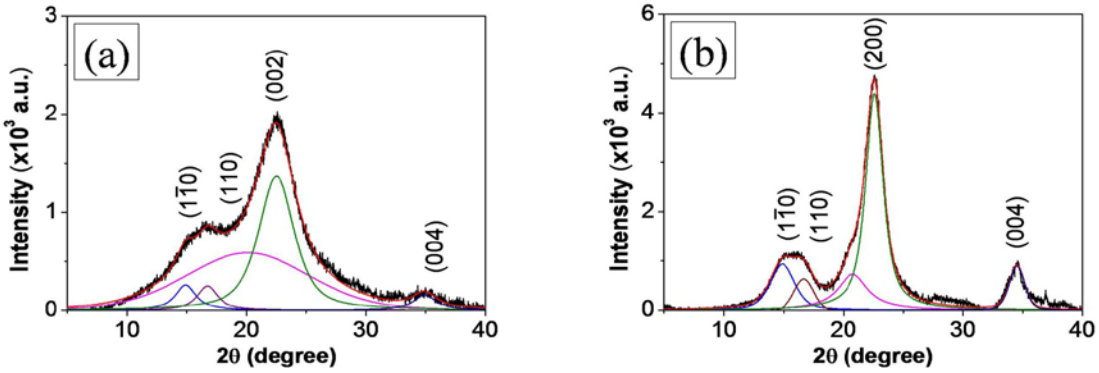

Figure 2: XRD patterns after deconvolution: (a) BFR and (b) BFA

Table 1
Crystallinity index and peak position from XRD analysis

Sample	Planes				CrI (%) from $[\frac{I_{cr}-I_{am}}{I_{cr}} \times 100]$	CrI (%) from area covered under I_{cr} and I_{am}	Crystal size from XRD (nm)
	1$\bar{1}$0	110	200	004			
	Peak positions (2θ) in degrees						
BFR	14.8	16.7	22.5	34.9	52.24	50.0	2.51
BFS	14.9	16.7	22.5	34.6	62.94	61.2	3.22
BFB	14.9	16.7	22.6	34.7	71.54	68.5	4.02
BFA	14.9	16.7	22.6	34.5	83.33	85.0	4.76

Fig. 1 (d)) and the presence of cellulose nanocrystallites could be seen clearly. The crystallinity of the samples obtained at different stages of extraction was calculated from the diffraction intensity data, using the empirical method for native cellulose.[14] The crystalline to amorphous ratio of the materials was determined using the formula:

$$\text{Cr.I}(\%) = \frac{I_{cr}-I_{am}}{I_{cr}} \times 100 \quad (1)$$

where I_{am} is the minimum diffraction intensity of the amorphous material taken at a 2θ angle between 19° and 20°, and I_{cr} is the maximum diffraction intensity of the (002) lattice peak at 2θ between 22° and 23° for crystalline cellulose.

It is apparent from the XRD studies that all the samples have cellulose I crystalline properties and possess high amorphous content. The deconvoluted peaks of a representative raw sample (BFR) and those of the crystalline material (BFA) are shown in Figure 2 (a) and Figure 2 (b), respectively. Using the intensity ratios of the peaks, as indicated in Equation (1), we have computed the crystallinity percentage in our samples and the results are given in Table 1. It may be seen that the crystalline content gradually increased as the extraction proceeded from the raw material (BFR) to the acid treated extracts (BFA). The acid hydrolyzed fibers (BFA) were richer in crystalline cellulose content than the raw fiber (BFR).

We have also computed the area under the peaks for the crystalline (I_{cr}) and amorphous (I_{am}) phases from the deconvoluted peaks for the representative raw sample (BFR) and for the crystalline (BFA) materials, as shown in Figure 2 (a) and Figure 2 (b), respectively. Their crystallinity values (%) calculated as stated above are shown in Table 1. These values indicate that the crystallinity gradually increased as the extraction process proceeded, starting from the raw material to the acid treated one. These values agree well with those obtained from intensity measurements.

Different cellulosic materials are known to have widely varying crystallite sizes.[23] Thus, it may be worthwhile now to determine the crystal sizes present in the cellulose material obtained at different extraction stages from the raw material using the well-known Scherrer equation,[24,25] which relates the crystallite size to the full width at half maximum (FWHM) as:

$$\tau = K\lambda/(\beta \text{Cos}\theta) \quad (2)$$

where τ is the size perpendicular to the lattice plane represented by the peak in question; the constant, K, is dependent on the crystal shape, while λ is the wavelength of the incident beam

used; β is the FWHM in radians and θ is related to the position of the peak.

The crystallite sizes obtained as described above ranged from 2.51 nm to 4.76 nm, and are listed in Table 1. It may be observed that the crystallite size increased significantly (nearly doubled) as the materials became more crystalline after acid treatment.

XPS studies

At this point, a critical analysis of the binding energy states of carbon in the extracts obtained at different stages of extraction may lead to a meaningful description of the changes occurring in the binding states within the cellulose material undergoing different stages of extraction. In general, the behavior of the extracts at different extraction stages appeared similar, therefore, we present here two of them as representative ones. The spectrum corresponding to the raw sample (BFR) is shown in Figure 3 (a), while the inset presents the spectrum for the crystalline one (BFA). Distinct peaks could be observed only for C1s and O1s. The core level spectra for C1s and O1s for the extracts obtained at different extraction stages are shown in Figure 3 (b-e).

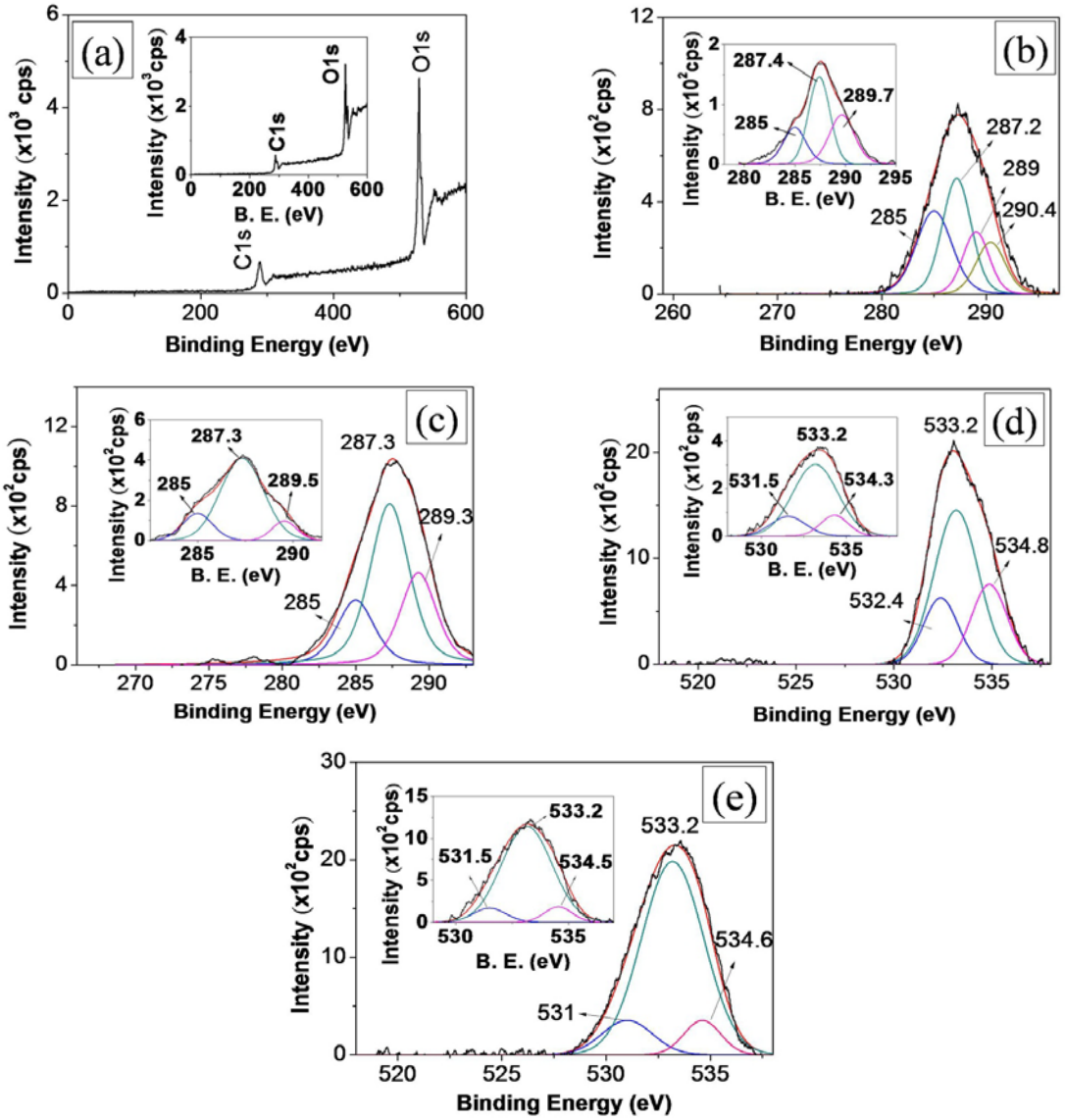

Figure 3: XPS spectra of banana fibers: survey scan of (a) BFR (inset shows the same for BFB), (b) C1s spectra of BFR (inset – BFS), (c) C1s spectra of BFB (inset – BFA), (d) O1s spectra of BFR (inset – BFS) and (e) O1s spectra of BFB (inset – BFA)

Table 2
Carbon content in the samples assessed by different methods

Sample	XPS		Raman		FTIR	
	C1/C2	O/C	I_D/I_G	Ratio of the area under D and G peaks	$X_c = I_{1428}/I_{898}$	sp^3/sp^2
BFR	0.89	0.48	0.48	1.63	0.59	5.25
BFS	0.49	0.57	1.01	0.84	0.62	13.5
BFB	0.15	0.79	1.34	1.44	0.69	23.2
BFA	0.09	0.79	2.24	0.79	0.83	36.24

The high resolution spectra of the C1s peak reveal the existence of at least three types of carbon bonds in all the samples. The C1s spectra for BFR (Fig. 3 (b)) around ~287.2 eV could be deconvoluted into four peaks located at ~285 eV for C1s-C sp^2, ~287.2 eV for C1s-OH and two peaks at higher binding energies at ~289 eV and 290.4 eV. The peak located at ~289.4 eV could be assigned to the satellite peak corresponding to the π-π* transition in the aromatic systems. These values matched well with those reported by Drewniak *et al*.,[26] Briggs *et al*.[27] and Stankovich *et al*.[28]

The alkali treated samples indicated (inset of Fig. 3 (b)) three peaks located at ~285 eV, 287.4 eV and 289.7 eV. Here again the main strong peak is due to a carbonyl group located at ~287.4 eV along with that at ~285 eV for C1s-C sp^2 and the satellite at ~289.5 eV corresponding to the π-π* transition. The core level C1s spectrum of the extract obtained after bleaching (BFB) is shown in Figure 3 (c). The bleached sample exhibited (Fig. 3 (c)) a strong peak at ~287.3 eV, indicating overlapping peaks at ~285 eV (C–O), ~287.3 eV (C1s-OH) and 289.3 eV (O–C–O). The acid treated extract (BFA) showed (inset of Fig. 3 (c)) a broader peak located at ~287.3 eV, which could also be deconvoluted into three peaks located at ~ 285 eV, 287.3 eV and 289.5 eV arising due to (C-O), (C1s-OH) and (O–C–O) bonds, respectively.

The modulation of the C1s peak with an increase in the crystallinity index will be apparent from the core level spectra of cellulose obtained at different stages of extraction. Hydrogen bonding would change as the relative amount of the amorphous and crystalline cellulose content is altered. This should be reflected from the modulation of binding energies of C1s in the cellulose materials obtained at different extraction stages. It is known that the characteristic C1s peaks of cellulose (C2) are located at ~287.3 eV and ~289.3 eV, while that for the non-cellulosic component (C1) is located at ~285 eV. The analysis of the peak area under the above-mentioned peaks would also reflect the crystallinity of the extracts. The results are shown in Table 2, indicating that the non-cellulosic component located at ~285 eV for the raw material (BFR) decreased significantly with the associated increase in the cellulosic component with subsequent chemical treatment, which is indicated by the ratios of C1s (285 eV)/C1s (287.3 eV). The highest amount of the cellulosic component was noted for the BFA samples.

The core level spectra of O1s for the cellulose extracted at different stages of extraction are illustrated in Figure 3 (d, e). These spectra could be resolved into three Gaussian components. The most intense peak was centered between 530 and 536 eV. The origin of the peaks could be associated with the electrons from the oxygen atoms bonded to hydrogen atoms (OH).[27,29,30] Another component located at a relatively higher energy, at ~534.8 eV (Fig. 3 (d)), for the raw sample (BFR) could be assigned to electrons from the oxygen atoms bonded to one carbon atom.[31] With further alkali (BFS) and acid (BFA) treatments, the intensity of this peak diminishes significantly (insets of Fig. 3 (d, e)). The third component located at lower energy, at ~531.5 eV, could be associated to the carbonyl groups C=O.[27] The core level spectra for the bleached samples (BFB) is shown in Figure 3 (e), indicating three peaks located at 531 eV, 533.2 eV and 534.5 eV. These peaks have a similar origin to that noted for the BFA samples. Oxygen to carbon ratios computed from the XPS data are also shown in Table 2. It may be observed that the C/O ratio increased in the cellulose material during successive treatments, with the highest value (0.79) for the acid hydrolyzed (BFA) material, which has a greater amount of crystalline cellulose. It may be noted here that this value compares well with the theoretical value (0.83).[32,33] The C1/C2 ratio decreased significantly when the raw (BFR) material was

finally acid hydrolyzed to obtain cellulose nanocrystals (BFA). This indicates that the cellulose nanocrystals are richer in sp^3 carbon content compared to other materials obtained from different extraction stages, such as the alkali treated (BFS) and the bleached (BFB) samples.

Raman studies

In Raman spectra, the region below 1700 cm^{-1} depicts the cellulose backbone. Strong and sensitive peaks are generally noted in the range of 100 cm^{-1} to 1700 cm^{-1}. The region above 2700 cm^{-1} is generally more sensitive to hydrogen bonding.[34,35] Full-range Raman spectra (50-4000 cm^{-1}) for two representative extracts – raw (BFR) and crystalline (BFA) materials – derived in the initial and final stages of extraction are shown in Figure 4 (a) and Figure 4 (b), respectively. It could be observed that, beyond 1700 cm^{-1}, the Raman spectra for all the cellulose materials investigated were nearly featureless (Fig. 4 (a)), except for BFA (Fig. 4 (b)). Therefore, only the spectra for BFR (Fig. 4 (a)) and BFA (Fig. 4 (b)) are presented here as representative ones. The Raman spectrum for the raw sample (BFR) exhibits low intensity peaks located at ~1098 cm^{-1}, 1165 cm^{-1}, 1265 cm^{-1}, 1338 cm^{-1} and 1607 cm^{-1}. The acid hydrolyzed extracts display additional peaks located at ~379 cm^{-1}, ~433 cm^{-1} and ~896 cm^{-1}. A peak located at ~2904 cm^{-1} can be ascribed to C-H/CH_2 stretching vibrations. No peak between 3200 cm^{-1} and 3500 cm^{-1}, which would correspond to OH stretching vibrations, is present in any of our samples. This would imply that all the samples were properly dried and kept in good dry condition.

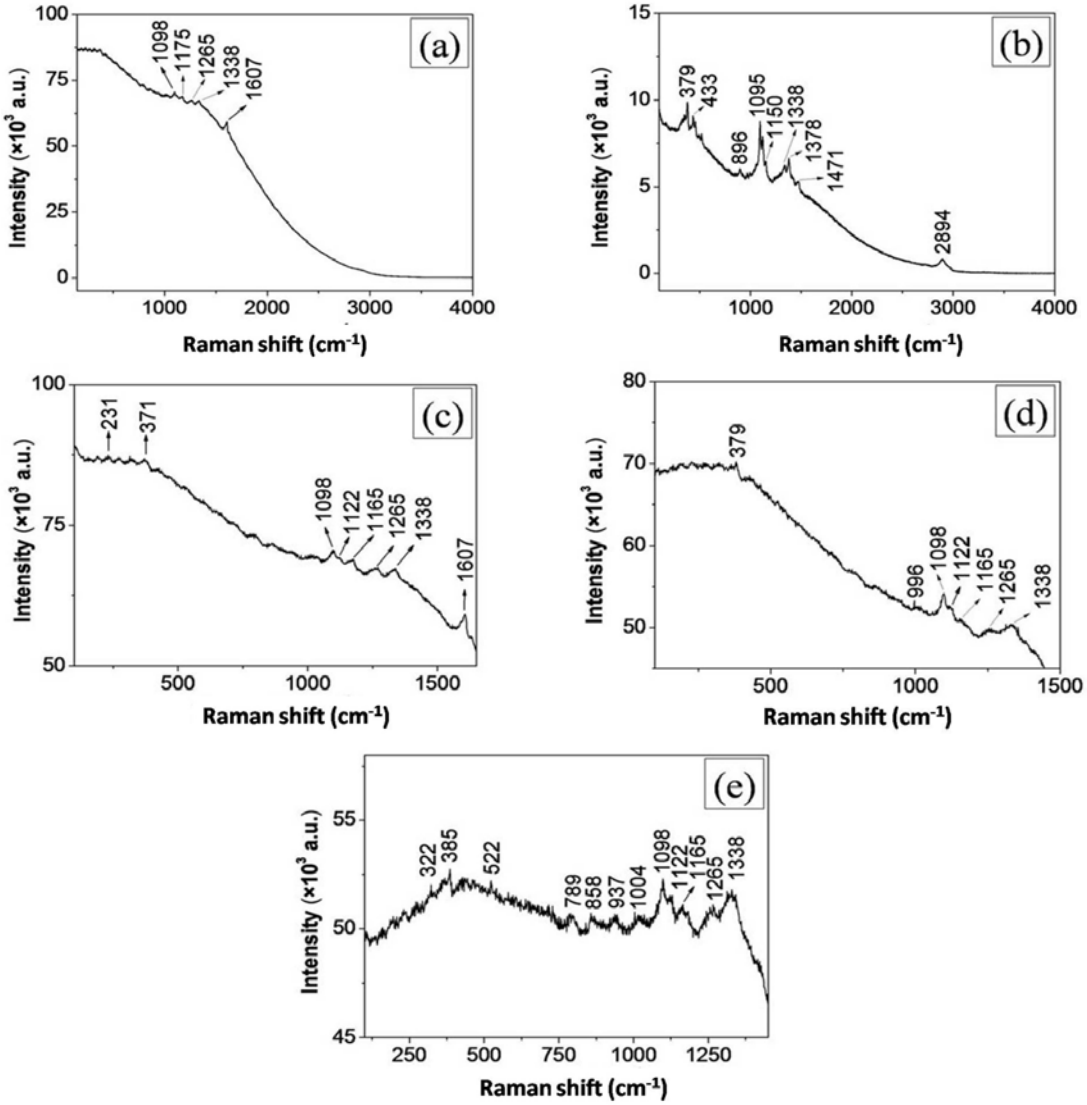

Figure 4: Raman spectra of banana fibers: full range scan of (a) BFR, (b) BFA; and selective range scan of (c) BFR, (d) BFS, (e) BFB and (f) BFA

It may be prudent to look into the details of the Raman spectra for all the cellulosic samples (BFR, BFS, BFB and BFA) recorded in the spectral range of 100-1700 cm^{-1} (Fig. 4 (c-f)). The peak intensities for the raw material (BFR) (Fig. 4 (c)) and the alkali treated extract (BFS) (Fig. 4 (d)) are significantly lower, compared to those for the bleached sample (BFB) (Fig. 4 (e)) and the acid treated sample (BFA) (Fig. 4 (f)). The peak at ~1316-1338 cm^{-1}, representing the H-O-C bending mode, is present in all the materials obtained at different stages of extraction. The peak at ~370-385 cm^{-1}, representing the characteristic mode for amorphous cellulose, is also present in all the samples with varying intensity[36,37] (Fig. 4 (c-f)). The skeletal bending modes of CCC, COC, OCC and OCO are generally dominant in the 150-550 cm^{-1} region. Methane bending (CCH, COH) and the movement of CC and CO groups within the glucopyranose ring units might be involved in such cases. One may observe the presence of the above Raman peaks in this 150-550 cm^{-1} region in all the samples with varied intensity. The most visible distinction in nanocrystalline cellulose in the 150-800 cm^{-1} region is the absence of peaks around 171 cm^{-1} and 258 cm^{-1}. This would probably indicate -COH bending.[34,38] The peak appearing in the region of ~860-1098 cm^{-1} could be ascribed to C-C and C-O stretching modes and some amounts of HCC and HCO bending modes. The above peaks became distinct and stronger for the acid treated sample (Fig. 4 (f)). The increase in intensity of the above peaks could be attributed to an increase in cellulose crystallinity and crystallite sizes. This observation is in conformity with the findings reported by Atalla and Wiley.[39] In Figure 4 (f), the peak for nanocrystalline cellulose is sharper and shifted to frequencies of ~896 cm^{-1}. In the 1270-1350 cm^{-1} region, the bending mode for HCC/HCO was observed (Fig. 4 (e, f)). In the 1350-1430 cm^{-1} region, the bending of COH was present. Figure 4 (c-f) also shows the presence of bands in the cellulose spectrum at ~850-950 cm^{-1}, ~1250-1262 cm^{-1} and ~1400-1472 cm^{-1}.[43]

One can locate a distinct peak in the spectral region of D-peak located at ~1330 cm^{-1} and G-peak located at ~1600 cm^{-1}. The G (graphite) peak at 1568 cm^{-1} is considered sensitive mainly to the configuration of sp^2 sites due to their higher cross section. Thus, the ratio (I_D/I_G) of the intensities of D-peak (I_D) and G-peak (I_G) would be a measure of the size of sp^2 phase organized in rings. The FWHM of the G-peak, arising from bond angle and bond length distortions, is generally sensitive to structural disorder. Thus, the FWHM of the G-peak would be small where the clusters were defect-free, unstrained or molecular. This would mean that a higher FWHM would indicate higher bond length and bond angle disorder. Thus, for a given cluster size, a higher FWHM would indicate the presence of higher sp^3 hybridized carbon content in the material.[40-43] The intensity ratio (I_D/I_G) may look like a very useful parameter in the Raman study. However, the ratio of the integrated areas covered under the D and G peaks was also reported to indicate the bonding environment by many researchers. The ratio of the areas under the D and G peaks is essentially equivalent to the product of the intensity ratio (I_D/I_G) and the FWHM of the D and G peaks. It may not be the best parameter to determine the sp^2/sp^3 ratio from the area covered under the D and G peaks, as indicated by Robertson.[43] It may be interesting to study the dependence of sp^2/sp^3 ratios on I_D/I_G and the area under the D and G peaks separately, since they might contain different information. We have computed the data above from the Raman spectra and the results are shown in Table 2. It could be seen that the sp^2 carbon content in the raw sample (BFR) was the highest, indicating more amorphous carbon content in the material. Samples became sp^3 hybridized carbon rich as the crystallinity in the cellulose increased with successive chemical treatment during the extraction of cellulose. BFA samples showed significantly higher sp^3 hybridized carbon content. It may also be noted that the results obtained from the intensity ratio (I_D/I_G) are quite systematic, compared to those obtained from the areas covered under the D and G peaks, which were quite inconsistent.

FTIR studies

FTIR spectra of the banana fibers at various stages of extraction (BFR, BFS, BFB and BFA) are shown in Figure 5. A broad absorption band in the region of 3400-3500 cm^{-1} was observed in all the samples, which is associated with the presence of –OH stretching vibration. Peaks associated with $–CH_2$ asymmetric stretching vibrations at ~2922 cm^{-1} were present in all the samples. This band is due to the C-H stretching in methyl and methylene group. The –CH symmetric stretching vibration peak is prominent only in BFB (trace c) and BFA (trace d). Absorption bands at ~1736 cm^{-1} and 1250 cm^{-1}, associated with C=O and

C−O stretching of the acetyl group due to hemicelluloses, are present only in the BFR (trace a) sample. The absence of these bands after alkali and acid treatments suggests (traces b, d) removal of the hemicelluloses present in the raw samples (BFR), implying the alkali treatment in the steam explosion process as the cause. The peak at ~1639 cm^{-1} present in all the samples could be attributed to O-H bending vibrations of absorbed water. The band at ~1461.9 cm^{-1} present only in BFR (trace a) could be attributed to C-H deformation of lignin and would suggest partial removal of lignin in the steam explosion process. The absorption bands near 1428 cm^{-1} and 1375 cm^{-1} are associated with $–CH_2$ symmetric bending and –CH symmetric deformation of cellulose, respectively. The peak at ~1162 cm^{-1} present in all the samples arose due to asymmetrical stretching of C−O−C present in cellulose and hemicelluloses. The peak is more prominent in BFB (trace c) and BFA (trace d) due to the gradual increase of the crystalline cellulose content. The absorption peaks at ~1110 cm^{-1} and ~1031 cm^{-1} in BFS, BFB and BFA are associated with the stretching of C−O−C and pyranose ring skeletal vibration of cellulose. The bands located in the region of 1047-1059 cm^{-1} correspond to C-O, and C=C, and C-C-O stretching in cellulose, hemicelluloses and lignin. The signature peak of β-glycosidic linkages of the cellulosic material is found at ~898 cm^{-1} in all the samples.[44]

Polymers with long, slender chains of glucopyranose units generally comprise cellulose. The formation of various kinds of inter- and intra-molecular hydrogen bonds is the contribution of the hydroxyl groups in each unit. The intermolecular H-bonding is between each glucopyranose unit, while the intramolecular bonding is between the -OH groups of fiber and the -OH groups of the matrix. The formation of inter- and intra-molecular hydrogen bonds in the cellulose has a strong influence on the physical properties of cellulose, including solubility, hydroxyl reactivity and crystallinity. They also modulate the mechanical properties of the cellulose-based composites. The crystallinity of cellulose is known to play a significant role on the physical, chemical and mechanical properties of cellulose-based composites. The tensile strength, compressive strength, storage modulus, thermal stability of composites *etc*. have been noted to enhance with increasing crystallinity of cellulose. Ciolacu *et al*.[44] determined the crystallinity of cellulose in treated cellulose fiber by comparing the intensities of the peaks located at ~1428 cm^{-1} and ~893 cm^{-1} from the FTIR spectra:

$$Xc = I_{1428}/I_{898} \quad (3)$$

where Xc is the degree of crystallinity of cellulose.

The FTIR absorption band at ~1428 cm^{-1} may be assigned to a symmetric CH_2 bending vibration. This band is also referred to as the “crystallinity band”. The FTIR absorption band at 898 cm^{-1} may be assigned to C–O–C stretching at β-(1→4)-glycosidic linkages, which may be distinguished as an “amorphous” absorption band. We have computed the above-mentioned ratio for cellulose at different stages of extraction. The values have been tabulated in Table 2. It may be observed that crystallinity increases significantly from 0.59 for BFR to 0.83 for BFA samples. This result is in agreement with that obtained from XRD measurements.

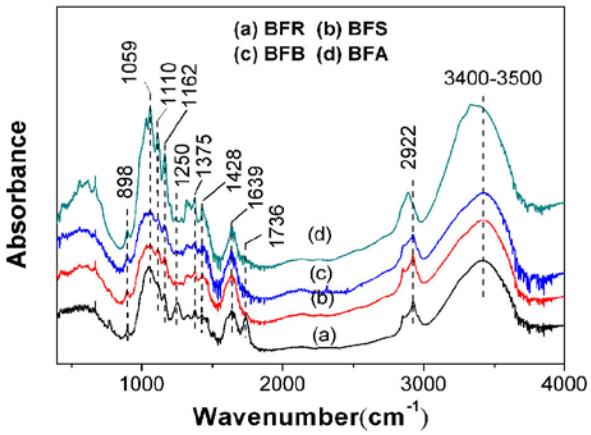

Figure 5: FTIR spectra of banana fiber: BFR, BFS, BFB and BFA

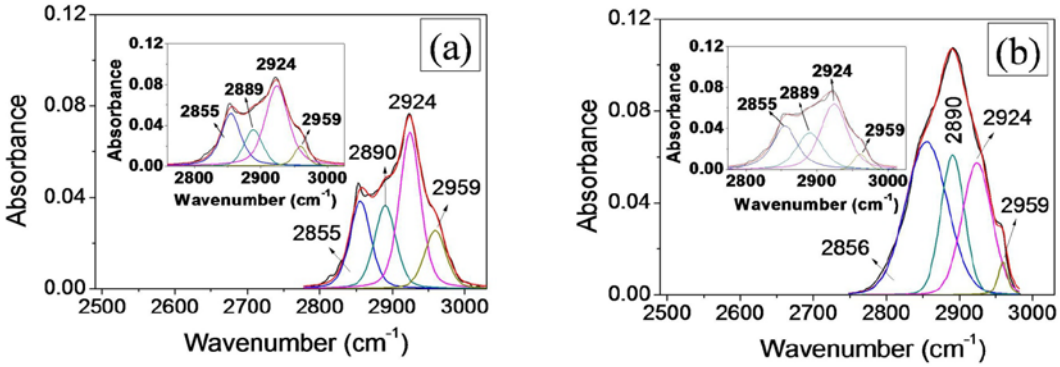

Figure 6: Deconvoluted FTIR spectra around 2950 cm^{-1} for: (a) BFR (inset shows the same for BFS), (b) BFA (inset shows the same for BFB)

The deconvolution of the peaks around 2900 cm^{-1} for representative samples of raw material (BFR) and acid treated crystalline material is shown in Figure 6 (a) and Figure 6 (b), respectively. Insets show the same for BFS and BFB samples. The spectra (Fig. 6) indicate the presence of four major peaks. The peaks may be related to different characteristic sp^3 and sp^2 C–H bonds with different stretch area under individual peaks. The peaks at ~2950 cm^{-1} and ~2920 cm^{-1}, related to sp^2 –CH olefinic group and sp^3 –CH symmetric modes, respectively, became distinct (Fig. 6 (b)). The shoulder at ~2860 cm^{-1} arising due to sp^3 –CH symmetric stretching vibrations also became prominent. IR measurement is not generally considered as a very accurate method for estimating the sp^3/sp^2 ratio in cellulose, since it only gives the amount of C-H bonds and not C-C bonds.[43,45] The accuracy of the method would depend on the resolution of the peaks for the C-H bonds. Thus, this method may not be suitable for determining the sp^3/sp^2 ratio in materials with low hydrogen content. In this measurement, we observed the peaks at ~2857 cm^{-1} and ~2920 cm^{-1}, which are generally related to sp^3 -CH olefinic group and sp^3-CH symmetric modes, respectively. However, it could be noted that the cellulose produced a very strong peak located at ~2959 cm^{-1}, related to sp^2-CH_2 symmetric stretching vibrations. This would imply that, upon extraction of cellulose, it becomes richer in sp^3 bonded carbon, as it proceeds through the stages BFR-BFS-BFB-BFA.

Nonetheless, a rough estimate of the sp^3/sp^2 ratio could be obtained from FTIR studies by calculating the area under the peaks associated with sp^3- and sp^2-bonded carbons. Peak deconvolution around 2950 cm^{-1} (Fig. 6) indicated the presence of four peaks. The peaks are related to different characteristic sp^3 and sp^2 C–H bonds with different stretch areas under individual peaks. The sp^3/sp^2 ratio was computed by taking cognizance of these peaks. The results are shown in Table 2. It may be remarked that this observation tallied well with those obtained from Raman measurements. The raw material (BFR) contained most of the sp^2 bonded carbon and the acid treated crystalline samples (BFA) contained most sp^3 bonded carbon. This observation is in agreement with those obtained from Raman and XPS measurements.

CONCLUSION

Cellulose fibers were successfully extracted from *Musa sapientum* and subjected to different treatments. Then, the obtained cellulose materials were characterized for better understanding their structure. The XRD spectra contained peaks at 2θ ~14.9°, 16.7°, 22.6° and 34.9°, corresponding to the (1$\bar{1}$0), (110), (200) and (004) crystallographic planes, respectively. It was observed that the acid hydrolyzed sample (BFA) was richer in crystalline cellulose content than the raw fiber (BFR). The crystallite sizes estimated from the XRD studies ranged from 2.51 nm to 4.76 nm. High-resolution XPS spectra of the C1s peak revealed the existence of three types of carbon bonds in all the samples. They were located at ~285 eV for C1s-C sp^2, ~287.2 eV for C1s-OH and at higher binding energies of ~289 eV. It was concluded from the XPS studies that the carbon content decreased in the samples with a larger amount of the cellulosic component. Raman studies established the highest sp^2 carbon content in the raw sample (BFR), indicating more amorphous carbon content in the material. Samples became sp^3 hybridized carbon rich as the crystallinity in the cellulose increased with

successive chemical treatments. BFA samples showed significantly higher sp^3 hybridized carbon content. FTIR peaks associated with $–CH_2$ asymmetric stretching vibrations near 2920 cm^{-1} were present in all the samples. The absorption bands at ~1736 cm^{-1} and 1250 cm^{-1}, associated with C=O and C−O stretching of the acetyl group due to hemicelluloses, were present only in the raw samples (BFR). It was observed that crystallinity increased significantly from 0.59 in BFR to 0.83 in BFA samples. It was also observed that upon extraction of cellulose, at different stages, cellulose became richer in sp^3 bonded carbon as it proceeded through the stages BFR-BFS-BFB-BFA.

ACKNOWLEDGEMENTS: One of the authors, D. Das, wishes to thank the Government of West Bengal, India, and UGC-DAE-CSR, the Government of India, for financial help through his fellowship.

REFERENCES

[1] R. A. Ilyas, S. M. Sapuana and M. R. Ishak, *Carbohyd. Polym.*, **181**, 1038 (2018).
[2] C. J. Chirayil, L. Mathew and S. Thomas, *Rev. Adv. Mater. Sci.*, **37**, 20 (2014).
[3] N. Abdullah, F. Sulaiman, M. A. Miskam and R. M. Taib, *Int. J. Food Agric. Vet. Sci.*, **8**, 712 (2014).
[4] U. J. Kim, S. H. Eom and M. Wada, *Polym. Degrad. Stabil.*, **95**, 778 (2010).
[5] S. M. Rosa, N. Rehman, M. I. G. de Miranda, S. M. Nachtigall and C. I. Bica, *Carbohyd. Polym.*, **87**, 1131 (2012).
[6] M. George, W. Shen, K. Sharma and C. Montemagno, *Cellulose Chem. Technol.*, **51**, 681 (2017).
[7] B. Hong, F. Chen and G. Xue, *Cellulose Chem. Technol.*, **50**, 225 (2016).
[8] E. Corradini, E. A. G. Pineda, A. C. Corrêa, E. M. Teixeira and L. H. C. Mattoso, *Cellulose Chem. Technol.*, **50**, 737 (2016).
[9] Y. Feng, T. Cheng, W. Yang, P. Ma, H. He *et al.*, *Ind. Crop. Prod.*, **111**, 285 (2018).
[10] K. Nisizawa, *J. Ferment. Technol.*, **51**, 267 (1973).
[11] R. H. Newman, *Solid State Nucl. Mag.*, **15**, 21 (1999).
[12] S. Park, D. K. Johnson, C. I. Ishizawa, P. A. Parilla and M. F. Davis, *Cellulose*, **16**, 641 (2009).
[13] K. Schenzel, S. Fischer and E. Brendler, *Cellulose*, **12**, 223 (2005).
[14] L. G. J. M. A. Segal, J. J. Creely, A. E. Martin Jr. and C. M. Conrad, *Text. Res. J.*, **29**, 786 (1959).
[15] C. Driemeier and G. A. Calligaris, *J. Appl. Crystallogr.*, **44**, 184 (2011).
[16] A. D. French, *Cellulose*, **21**, 885 (2014).
[17] A. D. French and M. S. Cintrón, *Cellulose*, **20**, 583 (2013).
[18] M. M. de Souza Lima and R. Borsali, *Macromol. Rapid. Comm.*, **25**, 771 (2004).
[19] M. P. Adinugraha and D. W. Marseno, *Carbohyd. Polym.*, **62**, 164 (2005).
[20] V. Favier, H. Chanzy and J. Y. Cavaille, *Macromolecules*, **28**, 6365 (1995).
[21] M. A. Spinacé, C. S. Lambert, K. K. Fermoselli and M. A. De Paoli, *Carbohyd. Polym.*, **77**, 47 (2009).
[22] L. A. Costa, A. F. Fonseca, F. V. Pereira and J. I. Druzian, *Cellulose Chem. Technol.*, **49**, 127 (2015).
[23] K. Leppänen, S. Andersson, M. Torkkeli, M. Knaapila, N. Kotelnikova *et al.*, *Cellulose*, **16**, 999 (2009).
[24] J. I. Langford and A. J. C. Wilson, *J. Appl. Crystallogr.*, **11**, 102 (1978).
[25] P. Scherrer, *Nachr. Ges. Wiss. Göttingen*, **2**, 96 (1918).
[26] S. Drewniak, R. Muzyka, A. Stolarczyk, T. Pustelny, M. Kotyczka-Moranska *et al.*, *Sensors*, **16**, 103 (2016).
[27] D. Briggs and G. Beamson, "High Resolution XPS of Organic Polymers: The Scienta ESCA300 Database", John Wiley & Sons Inc., New York, 1992.
[28] S. Stankovich, R. D. Piner, X. Chen, N. Wu, S. T. Nguyen *et al.*, *J. Mater. Chem.*, **16**, 155 (2006).
[29] S. Danielache, M. Mizuno, S. Shimada, K. Endo, T. Ida *et al.*, *Polym. J.*, **37**, 21 (2005).
[30] L. J. Matienzo and S. K. Winnacker, *Macromol. Mater. Eng.*, **287**, 871 (2002).
[31] G. Shen, M. F. G. Anand and R. Levicky, *Nucleic Acid. Res.*, **32**, 5973 (2004).
[32] G. M. Dorris and D. G. Gray, *Cellulose Chem. Technol.*, **12**, 9 (1978).
[33] G. M. Dorris and D. G. Gray, *Cellulose Chem. Technol.*, **12**, 721 (1978).
[34] J. H. Wiley and R. H. Atalla, *Carbohyd. Res.*, **160**, 113 (1987).
[35] J. H. Wiley, PhD Dissertation, Institute of Paper Chemistry, Appleton, WI, USA, 1986.
[36] L. C. Li, *Forensic Sci. J.*, **6**, 55 (2007).
[37] K. Schenzel and S. Fischer, *Biomaterials*, **1**, 9 (2004).
[38] K. Schenzel and S. Fischer, *Cellulose*, **8**, 49 (2001).
[39] R. H. Atalla and J. H. Wiley, IPC Technical Paper Series No 226, Institute of Paper Chemistry, Appleton, WI, USA, 1987.
[40] C. Casiraghi, A. C. Ferrari and J. Robertson, *Phys. Rev. B.*, **72**, 85401 (2005).
[41] A. C. Ferrari and J. Robertson, *Phys. Rev. B.*, **61**, 14095 (2000).
[42] J. Filik, *Spectroscopy Europe*, **17**, 10 (2005).
[43] J. Robertson, *Mater. Sci. Eng. R. Rep.*, **37**, 129 (2002).
[44] D. Ciolacu, F. Ciolacu and V. I. Popa, *Cellulose Chem. Technol.*, **45**, 13 (2011).
[45] A. Grill and V. Patel, *Appl. Phys. Lett.*, **60**, 2089 (1992).